

## Discriminating between $\nu_\mu \leftrightarrow \nu_\tau$ and $\nu_\mu \leftrightarrow \nu_{sterile}$ in atmospheric $\nu_\mu$ oscillations with the Super-Kamiokande detector.

A. Habig

University of Minnesota Duluth

**Abstract.** A strong body of evidence now exists for atmospheric  $\nu_\mu$  disappearance oscillations. Such disappearance could be explained by oscillations to either  $\nu_\tau$  or a “sterile” neutrino ( $\nu_s$ ). Super-Kamiokande uses three different methods to distinguish between these two scenarios. First, matter effects would suppress the  $\nu_\mu \leftrightarrow \nu_s$  oscillation amplitude at high energy. Second, oscillation to  $\nu_s$  would reduce the overall neutral-current neutrino interaction rate. Third, the smoking gun of  $\nu_\mu \leftrightarrow \nu_\tau$  oscillations would be the observation of  $\tau$  appearance resulting from charged-current  $\nu_\tau$  interactions. The results of these three techniques are presented, which strongly favor  $\nu_\mu \leftrightarrow \nu_\tau$  oscillations over  $\nu_\mu \leftrightarrow \nu_s$ .

### 1 Introduction

The Super-Kamiokande (Super-K) experiment has reported evidence for the oscillation of muon neutrinos produced in cosmic-ray induced showers in the atmosphere, via the observation of  $\nu_\mu$  disappearance as a function of neutrino path-length and energy (Y. Fukuda *et al.*, 1998, 1999). The observed  $\nu_e$  signal shows no excess, so is not consistent with substantial  $\nu_\mu \leftrightarrow \nu_e$  oscillation; therefore the missing  $\nu_\mu$  must be changing to an “invisible” flavor. Since a  $\nu_\tau$  charged-current (CC) interaction would produce a  $\tau$  lepton,  $\nu_\tau$  below the 3.4 GeV  $\tau$  production threshold do not interact via the CC channel.  $\nu_\tau$  above this threshold would produce  $\tau$  leptons, but  $\tau$  decay products would produce a multiplicity of particles. Since the data set used to observe  $\nu_\mu$  oscillation selects only single-particle events, only the resulting disappearance of  $\nu_\mu$  is thus observed.

An alternative scenario that can explain muon neutrino disappearance is oscillation with a sterile neutrino ( $\nu_s$ ), which undergoes neither CC nor neutral current (NC) interactions. A fourth flavor of neutrino must be invoked to simultaneously explain apparent neutrino oscillations in three widely separated regimes: atmospheric neutrinos; solar neutrinos

(Bahcall *et al.*, 1998); and the LSND experiment (C. Athanassopoulos *et al.*, 1998). However, studies of the  $Z^0$  at LEP (Decamp *et al.*, 1992) indicate that any such new light neutrino flavor must not interact via the weak force, leading to speculation about a sterile flavor.

Super-K has used two methods to distinguish between the  $\nu_\tau$  and  $\nu_s$  hypotheses for explaining atmospheric  $\nu_\mu$  disappearance (Y. Fukuda *et al.*, 2000). The first method is to examine events likely to have been caused by NC interactions. While  $\nu_\tau$  readily undergo such interactions,  $\nu_s$  would not, resulting in a relative suppression of the NC signal. The second method exploits so-called “matter effects”, which reduce the oscillation amplitude of high-energy  $\nu_\mu \leftrightarrow \nu_s$  in the presence of matter (Liu *et al.*, 1998). While the combination of these two analyses disfavors  $\nu_\mu \leftrightarrow \nu_s$  compared with  $\nu_\mu \leftrightarrow \nu_\tau$ , the observation of appearance of the newly created  $\nu_\tau$  would be a definitive answer. Presented here are an update to the NC and matter effect analyses and recent attempts to resolve such  $\nu_\tau$  appearance.

### 2 Data Analysis

Super-K is a 50 kt water Cherenkov detector employing 11,146 photomultiplier tubes (PMTs) to monitor an internal detector (ID) fiducial volume of 22.5 kilotons. Entering and exiting charged particles are identified by 1885 PMTs in an optically isolated outer volume (OD). Details of the detector, calibrations, and data reduction can be found in (Y. Fukuda *et al.*, 1998, 1999). Fully-contained (FC) events deposit all of their Cherenkov light in the ID while partially-contained (PC) events have exiting tracks which deposit some light in the OD. The vertex position, number of Cherenkov rings, ring directions, and momenta are reconstructed and the particle types are identified as “ $e$ -like” or “ $\mu$ -like” for each Cherenkov ring. In the current 79.4 kiloton-year (1289 day) FC sample, there are 3490 single-ring  $e$ -like events, 3346 single-ring  $\mu$ -like events and 3477 multi-ring events.

Based on 1268 live days, this detector has also collected

1416 upward through-going muon (UTM) events produced by atmospheric neutrino interactions in the surrounding rock. We required a minimum track length of 7 m in the inner detector and an upward muon direction. Downward-going neutrino induced muons cannot be distinguished from the 3 Hz of cosmic ray muons.

### 2.1 Observing $\nu_\mu$ disappearance

The FC single-ring data sample was analyzed to establish the region in  $(\sin^2 2\theta, \Delta m^2)$  oscillation parameter space where  $\nu_\mu$  disappearance is taking place. This data sample is dominated by quasi-elastic neutrino interactions, which allow the tagging of the flavor of the parent neutrino via the flavor of the observed outgoing lepton. Data was binned by energy, outgoing lepton flavor, and zenith angle of the lepton. The distance the neutrino has traveled can be inferred from the zenith angle, with those neutrinos coming from above having traveled only tens of km, and those coming from below the whole diameter of the earth. To provide an expected signal, 70 live-years equivalent of Monte-Carlo (MC) data was used. As published by Y. Fukuda *et al.* (1998), the number of observed  $\mu$ -like events in bins with low energies and long baselines is suppressed compared with the non-oscillated MC expectations.

To evaluate the suitability of possible oscillation parameters, a MC expectation was calculated using the oscillation probability appropriate for both two-flavor  $\nu_\mu \leftrightarrow \nu_\tau$  and  $\nu_\mu \leftrightarrow \nu_s$  oscillations. A  $\chi^2$  comparison of these MC predictions and the FC single-ring data yielded allowed regions in  $(\sin^2 2\theta, \Delta m^2)$  parameter space for both types of  $\nu_\mu$  disappearance oscillations. For the case of  $\nu_\mu \leftrightarrow \nu_s$ , matter effects were included, although at the  $\sim 1$  GeV neutrino energies in this data sample the matter effects are small and the two resulting allowed regions very similar. This analysis results in two sets of neutrino oscillation parameters which are consistent with  $\nu_\mu$  disappearance oscillations for a  $\nu_\tau$  oscillation partner or a  $\nu_s$ . For details of this fit see Y. Fukuda *et al.* (2000).

### 2.2 Neutral Current Sample

A set of cuts were devised to isolate a comparatively NC rich data set. These events must be contained, neutrino-induced events with multiple rings, the brightest of which must be identified as an electron. Furthermore, to improve the angular correlation of the observed particles to their parent neutrino, the total visible energy must be greater than 400 MeV. This results in a mean angle difference between the parent neutrino and the reconstructed event direction of  $33^\circ$ . When tested on the MC data, these cuts produce a data sample containing a 29% fraction of NC events. The FC single ring sample discussed above contains only  $\sim 6\%$  NC events. Figure 1(a) shows the zenith angle distribution of these events with predictions from the MC.

Since  $\nu_s$  do not interact via a NC channel, if the  $\nu_\mu$  are changing into  $\nu_s$  given sufficient distance to do so then the

long-pathlength zenith angle bins coming from below will have comparatively fewer NC events and the ratio of up-to-down events will be reduced. However,  $\nu_\tau$  do interact via the NC channel. Thus, if the explanation of the mu-like event suppression observed in the FC data is that  $\nu_\mu$  are changing to  $\nu_\tau$ , then the NC event rate coming up from below will remain unchanged, as will the up/down ratio of NC events.

We define ‘‘upward’’ as a cosine of zenith angle less than  $-0.4$  and ‘‘downward’’ as greater than  $+0.4$ . There are 465 upward events and 438 downward events in the NC-enriched sample. Figure 1(b) shows the  $\Delta m^2$  dependence of the expected up/down ratio in the case of full mixing ( $\sin^2 2\theta = 1$ ). For  $\Delta m^2 = 3.2 \times 10^{-3} \text{ eV}^2$ , the data are consistent with  $\nu_\mu \leftrightarrow \nu_\tau$ , while the up/down ratio predicted by  $\nu_\mu \leftrightarrow \nu_s$  oscillations is  $3.4\sigma$  too low.

Using this up-to-down ratio helps to cancel some systematic uncertainties, particularly the rather large uncertainties in the NC cross-sections. The total systematic uncertainty in the up/down ratio of the data and MC is estimated to be  $\pm 2.9\%$  (Y. Fukuda *et al.*, 2000).

### 2.3 Partially Contained Sample

To look for the presence of matter effects upon the oscillation amplitude, we turn to a higher energy event sample as matter effects are strongest at high energies. The partially contained (PC) event sample is created by neutrino interactions in the fiducial volume of water which produce an outgoing particle with a high enough energy to escape the inner detector. PC events in Super-K are estimated to be 97% pure  $\nu_\mu$  CC and result from parent neutrinos with a mean of 10 GeV. A further requirement of a visible energy of greater than 5 GeV raises this mean neutrino energy to 20 GeV. Figure 1(c) shows the zenith angle distribution of these events with predictions from MC, as before. Again an up/down ratio is employed to cancel systematic uncertainties using the same angular definition as for the multi-ring sample. There are 46 ‘‘up’’ events and 90 ‘‘down’’ events. Figure 1(d) shows the  $\Delta m^2$  dependence of the expected up/down ratio in the case of full mixing. Since matter effects suppress oscillations to  $\nu_s$ , the up/down ratio would remain near one in the case of  $\nu_\mu \leftrightarrow \nu_s$  oscillations. However, for  $\Delta m^2 = 3.2 \times 10^{-3} \text{ eV}^2$ , the observed up/down ratio is consistent with  $\nu_\mu \leftrightarrow \nu_\tau$  oscillations and  $2.9\sigma$  too low for  $\nu_\mu \leftrightarrow \nu_s$ . The total systematic uncertainty in the up/down ratio is estimated to be  $\pm 4.1\%$ .

### 2.4 Upward Through-going Muon Sample

An even higher energy sample of neutrinos is observed by Super-K and produces upward through-going muon events. These neutrinos interact in the rock below Super-K and produce an outgoing muon with enough energy to reach and completely traverse the detector. The neutrinos which produce such events have a peak energy of 100 GeV, maximizing any possible matter effect suppression of oscillation amplitudes. Due to the down-going presence of cosmic ray muons, a ‘‘vertical’’ ( $\cos \theta < -0.4$ ) to ‘‘horizontal’’ ( $-0.4 < \cos \theta <$

–0) ratio is used to probe this sample. Figure 1(e) shows the zenith angle distribution of these events with predictions. Figure 1(f) shows the  $\Delta m^2$  dependence of the expected vertical/horizontal ratio in the case of full mixing. At the point of  $\Delta m^2 = 3.2 \times 10^{-3} \text{ eV}^2$ , the data are consistent with  $\nu_\mu \leftrightarrow \nu_\tau$  oscillation, while the predicted suppression of oscillations via the matter effect on  $\nu_\mu \leftrightarrow \nu_s$  oscillations is again not seen at a significance of  $2.9\sigma$ . We estimated the total systematic uncertainty in the horizontal/vertical flux ratio to be  $\pm 3.3\%$ .

### 2.5 Evaluating $\nu_\mu \leftrightarrow \nu_\tau$ versus $\nu_\mu \leftrightarrow \nu_s$

All four data samples discussed (FC single ring, NC, PC, and UTM) are independent. No data found in one is present in another. Thus, the results of the four can be statistically combined to address the question of  $\nu_\tau$  versus  $\nu_s$ . The FC data sample sets the allowable range of  $(\sin^2 2\theta, \Delta m^2)$  that fit the observed  $\nu_\mu$  disappearance oscillations for both  $\nu_\tau$  and  $\nu_s$ . Each pair of oscillation parameters in those allowed regions is used to generate an expected neutrino signal for each of the other three samples. This allows a comparison between the up/down or vertical/horizontal ratios observed in each of the three samples and that expected for both hypotheses. The data samples being independent, the sum of the squares of the three deviations between data and expectations should follow a  $\chi^2$  distribution with three degrees of freedom. A  $(\sin^2 2\theta, \Delta m^2)$  pair is disfavored at the 90(99)% C.L. if the value of the sum is greater than 6.3(11.3). For the case of  $\nu_\mu \leftrightarrow \nu_s$ , all parameters allowed at 99% C.L. by the FC single-ring  $\nu_s$  case are disfavored by least the 99% C.L. when the other three data sets are examined. However, all oscillation hypotheses in the  $\nu_\mu \leftrightarrow \nu_\tau$  FC 90% C.L. allowed region remain allowed by the three additional data sets.

### 2.6 Evaluating $\nu_\mu \leftrightarrow (\nu_\tau + \nu_s)$

While the above analysis disfavors pure  $\nu_\mu \leftrightarrow \nu_s$  oscillations,  $\nu_s$  could still be present as a sub-dominant partner in dominant  $\nu_\mu \leftrightarrow \nu_\tau$  oscillations if  $\nu_\tau$  and  $\nu_s$  form a close mass doublet (Fogli *et al.*, 2001). To test the extent of such mixing which would produce an expectation which remains compatible with the observed Super-K data, a global  $\chi^2$  was formed between all the atmospheric neutrino data present in Super-K (FC, PC, UTM, multi-ring NC, multi-ring  $\mu$ -like, and upward-stopping muons) and MC expectations including the appropriate level of  $\tau$  appearance and matter effects. Systematic errors were treated in a similar fashion to Y. Fukuda *et al.* (1998).

This global fit has 190 degrees of freedom. A pure  $\nu_\tau$  oscillation partner produces expectations which have a  $\chi^2$  difference from the data of 175.0 at the best fit point. Pure  $\nu_s$  as the oscillation partner yields  $\chi^2 = 204.8$  at its best fit, and is disfavored by  $> 5\sigma$  compared to pure  $\nu_\tau$ . If the fraction of  $\nu_s$  present in the oscillation sample ( $\sin^2 \xi$ ) is varied between these extremes such that  $\nu_\mu \rightarrow (\cos \xi \nu_\tau + \sin \xi \nu_s)$ , the maximum fraction of  $\nu_s$  allowed at the 90(99)% C.L. by the complete set of Super-K data is  $\sin^2 \xi = 25(35)\%$ . Thus, it is

still possible for  $\nu_s$  to be present in the atmospheric neutrino oscillations as a sub-dominant partner.

## 3 $\tau$ Appearance Searches

In contrast to looking for (and failing to find) hints of  $\nu_s$ , one could directly detect the presence of the newly created  $\nu_\tau$  by observing the  $\tau$  appearance associated with a  $\nu_\tau$  interaction. This is difficult, because the  $\tau$  itself has such a short lifetime that one must look for its decay products and then deduce that a  $\tau$  was their parent. Such events are both rather complicated and comparatively rare, as only a small component of the atmospheric neutrino spectrum exceeds the 3.4 GeV  $\tau$  production threshold. Around 75 such interactions are expected to be in the existing data set. Additionally, neutrino interactions which produce a number of pions or other mesons can mimic a  $\tau$  decay within the finite resolution of the Super-K detector. However, three separate analyses have looked for  $\tau$  appearance in Super-K, concentrating on hadronic decay modes. All three were developed using the existing atmospheric neutrino MC as background with a  $\tau$  signal injected. To evaluate their expected sensitivity, the resulting analyses were also applied to a MC atmospheric neutrino sample with  $\tau$  included at the level of maximal mixing and  $\Delta m^2 = 3.0 \times 10^{-3}$ , the remaining range of allowable oscillation parameters being considered here as a systematic error.

The first analysis makes use of the standard Super-K event reconstruction tools, which use likelihood calculations to compute to what degree the observed light pattern matches the expected distribution for a given set of particles. To isolate  $\tau$  events, cuts are imposed on the visible energy, number of rings, number of decay electrons, the fraction of energy in the brightest ring, the distance from the first ring to the decay electron, the max muon momentum, the transverse momentum, and the particle ID of the brightest ring.

The second analysis makes use of a neural-net algorithm, using variables obtained from the likelihood-based tools as input: number of rings found; number of seeds used as the input to the ring counting algorithm; number of decay electrons; particle ID of most energetic ring; number of muons; and visible energy. The net was trained and tested on  $\tau$  MC data and asked to classify data events as  $\tau$  or not.

The third analysis makes use of the fact that a  $\tau$  produced near threshold will decay symmetrically, while a non- $\tau$  pion-production event will have remaining momentum and skew the resulting particles in one direction. Thus, energy flow and jet-finding calculations are made in addition to initial cuts from the standard likelihood analysis.

After development and testing using the MC data as inputs, the analyses were then applied to the atmospheric neutrino data set. The events were binned into five bins in  $\cos \Theta$ , since if  $\nu_\tau$  are being created via oscillations they will be coming upward (at long pathlengths). A comparison between the data, the MC expectations with no  $\tau$  appearance included, and with an expectation including  $\tau$  appearance was made. The significances of the potential  $\tau$  excess are around  $2\sigma$

Analysis	$\varepsilon_\tau$	fit # $\tau$	$\sigma_{exp}$	$\sigma$
Likelihood	43%	$66 \pm 41_{stat}^{+25}_{-18}$	2.0	1.5
Neural Net	51%	$92 \pm 35_{stat}^{+17}_{-23}$	2.0	2.2
Energy Flow	32%	$79^{+44}_{-40}(stat + sys)$	1.9	1.8

**Table 1.**  $\tau$ -appearance analyses, their efficiencies at saving  $\tau$  events, the number of  $\tau$  they observed, and the expected and observed significances of the signals.

for all three analyses. A fit to the amount of  $\tau$  appearance which best describes the data yields the number of observed  $\tau$  shown in Tab. 1. These three analyses are highly correlated, so one cannot combine their results in any statistically meaningful way. While all three are consistent with the presence of  $\tau$  appearance, none are statistically significant.

#### 4 Summary and Conclusion

Three independent data samples are presented that discriminate between the oscillations to either  $\nu_\tau$  or  $\nu_s$  in the region of  $(\sin^2 2\theta, \Delta m^2)$  parameter space favored by the majority of the Super-K data. While two-flavor  $\nu_\mu \leftrightarrow \nu_s$   $\nu_\mu \leftrightarrow \nu_\tau$  oscillations both fit the low energy charged current data, the pure  $\nu_s$  hypothesis does not fit the higher energy and neutral current samples. Pure  $\nu_\mu \leftrightarrow \nu_\tau$  neutrino oscillations do fit all of the data samples presented, although a simultaneous fit to all available Super-K atmospheric neutrino data allows up to a 25% (90% C.L.) contribution from  $\nu_s$  as a sub-dominant oscillation partner. Additionally, searches for the  $\tau$  appearance associated with  $\nu_\mu \leftrightarrow \nu_\tau$  oscillations result in signals which are consistent with the presence of  $\tau$  appearance in the Super-K detector.

*Acknowledgements.* We gratefully acknowledge the cooperation of the Kamioka Mining and Smelting Company. The Super-K experiment was built and has been operated with funding from the Japanese Ministry of Education, Science, Sports and Culture, and the United States Department of Energy. We gratefully acknowledge individual support by the National Science Foundation and Research Corporation's Cottrell College Science Award.

#### References

- Y. Fukuda *et al.*, Phys. Rev. Lett. **81**, 1562 (1998).  
Y. Fukuda, *et al.*, Phys. Rev. Lett. **82**, 2644 (1999); Phys. Lett. B **467**, 185 (1999).  
J.N. Bahcall, P. I. Krastev, & A.Yu. Smirnov, Phys. Rev. D **58**, 096016 (1998).  
C. Athanassopoulos *et al.*, Phys. Rev. Lett. **81**, 1774 (1998).  
D. Decamp *et al.*, Z. Phys. C **35**, 1 (1992); P. Abreu *et al.*, Nucl. Phys. B **367**, 511 (1992); B. Adeva *et al.*, Z. Phys. C **51**, 179 (1991); G. Alexander *et al.*, Z. Phys. C **52**, 175 (1992).  
Y. Fukuda *et al.*, Phys. Rev. Lett. **85**, 3999 (2000).  
Q.Y. Liu, S.P. Mikheyev, & A.Yu. Smirnov, Phys. Lett. B **440**, 319 (1998) and many other references cited therein.  
G.L. Fogli, E. Lisi, A. Marrone, Phys. Rev. D **63**, 053008 (2001).

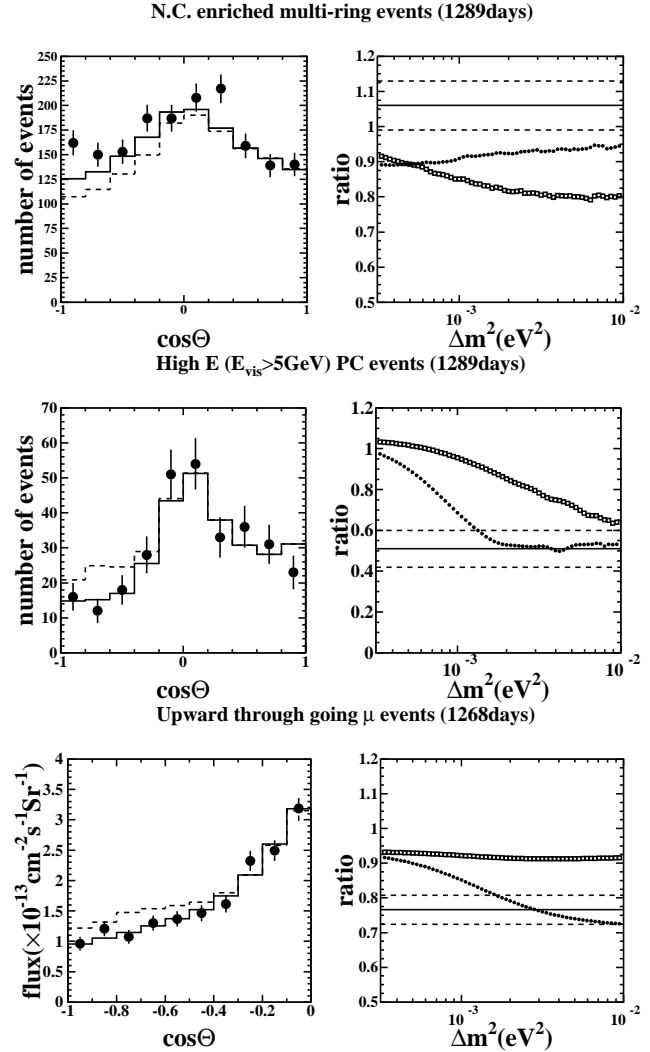


**Fig. 1.** (a,c,e) Zenith angle distributions of atmospheric neutrino events satisfying cuts described in the text: (a) multi-ring sample, (c) partially contained sample, and (e) upward through-going muon sample. The black dots indicate the data and statistical errors. The solid line indicates the prediction for  $\nu_\mu \leftrightarrow \nu_\tau$ , and the dashed for  $\nu_\mu \leftrightarrow \nu_s$ , with  $(\Delta m^2, \sin^2 2\theta) = (3.2 \times 10^{-3} \text{ eV}^2, 1)$ . The two predictions are independently normalized to the number of downward-going events for (a) and (c) and the number of horizontal events for (e). (b,d,f) Expected value of the corresponding test ratio as a function of  $\Delta m^2$ . The solid horizontal lines indicate the measured value from the Super-K data with statistical uncertainty indicated by dashed lines. Black dots indicate the prediction for  $\nu_\mu \leftrightarrow \nu_\tau$ , and empty squares for  $\nu_\mu \leftrightarrow \nu_s$ , in both cases for maximal mixing.